The Aeronautical Journal (2024), **128**, pp. 1344–1361
doi:10.1017/aer.2024.22

ROYAL AERONAUTICAL SOCIETY

RESEARCH ARTICLE

Water extraction in aero gas turbines for contrail mitigation

X. Gao , A. Isoldi, D. Nalianda and T. Nikolaidis

Centre for Propulsion and Thermal Power Engineering, Cranfield University, Cranfield, Bedfordshire, UK
Corresponding author: A. Isoldi; Email: a.isoldi@cranfield.ac.uk

Received: 29 October 2023; **Revised:** 13 February 2024; **Accepted:** 23 February 2024

Keywords: Aircraft emission; condensation trail; contrails; radiative forcing; water extraction; contrail mitigation

Abstract

Water vapour and particles in aero engine exhaust can give rise to condensation trails (contrails) in the wake of aircrafts, and recent studies suggest that persistent contrails and contrail cirrus account for circa 50% of the total aviation-derived radiative forcing (RF). The Schmidt-Appleman criterion is widely used to qualitatively predict the formation of contrails. The criterion indicates that the formation of contrails is affected by both aero engine exhaust and ambient air conditions and can therefore provide the theoretical basis to devise contrail mitigation strategies and further allows quantitative assessment of these strategies. This work focuses on water extraction from the aircraft engine exhaust for contrail mitigation. The fuel water emission index (EI_{H_2O}) is one of the key factors that determines whether persistent contrails form or not. It indicates the amount of water produced for every kg of fuel burnt. Research has indicated that water extraction from the exhaust of the aero engine has been considered for Nitrogen oxides (NOx) reduction, but not for contrail mitigation. Assuming that water extraction is indeed possible, the emphasis of this work will therefore be on understanding how much water is needed to be extracted for contrail mitigation depending on the altitude and the relative humidity (RH), with the aim to carry out a meaningful study on the mitigation of persistent contrails and contrail cirrus to enable a fast and considerable reduction in aviation-derived RF.

Nomenclature

AIC	aircraft-induced cloudiness
CU	Cranfield University
CO_2	carbon dioxide
EHV ($MJ * kg^{-1}$)	equivalent heat value
ERF ($mW * m^{-2}$)	effective radiative forcing
HHV ($MJ * kg^{-1}$)	higher heat value
LC	liquid critical
LEAP	leading edge aviation propulsion
LHV ($MJ * kg^{-1}$)	lower heat value
LM	liquid maximum
NO_x	nitrogen oxides
RF ($mW * m^{-2}$)	radiative forcing
RH	relative humidity
SFC ($kg * s^{-1} * kN^{-1}$)	specific fuel consumption
TAS ($m * s^{-1}$)	true air speed

A version of this paper first appeared at the 26th Conference of the International Society for Air Breathing (ISABE), 22–27 September 2024, Toulouse, France.

https://doi.org/10.1017/aer.2024.22 Published online by Cambridge University Press

Symbols

$c_P\ (J * kg^{-1} * K^{-1})$	air specific heat capacity
$e_{sat,l}\ (Pa)$	water vapour saturation pressure with respect to liquid water
EI_{H_2O}	fuel water emission index
$G\ (Pa * K^{-1})$	contrail factor
$p\ (Pa)$	atmospheric pressure
$Q\ (MJ * kg^{-1})$	fuel heat value
$T(K)$	static temperature
ε	water/air molar mass ratio
η	engine overall efficiency
λ	water extraction percentage

1.0 Introduction

1.1 Contrails radiative forcing

Aircraft can create thin line-shaped ice-clouds at high altitudes in specific environmental conditions in the upper troposphere (8–14km), called *contrails*, which is the abbreviation of condensation trails. If contrails can last for more than 10 minutes, they are referred to as persistent contrails, or long-lived contrails; otherwise, they are classified as non-persistent contrails, or short-lived contrails [1]. If persistent contrails spread and cover a large area, no longer retaining their linear shape, they become contrail cirrus [2]. Contrails formed at high altitudes reflect a small fraction of incoming solar radiation, but a large fraction of outgoing terrestrial radiation, thereby causing a perturbation of the Earth's radiation balance, giving a net positive radiative forcing (RF). Global RF cannot be measured directly, so it is usually estimated by models or extrapolation of regional values observed by satellites [3]. Contrails can be classified as a kind of artificial cloudiness; therefore, their impact on the Earth's radiation budget can be analysed and compared with other types of clouds. Cloudiness can be classified in three main types [4]:

- **Cloud-free atmosphere:** The gaseous molecules and aerosol particles absorb and scatter radiation from the sun and Earth's surface, causing a positive RF due to long-lived greenhouse gases accumulated in the atmosphere.
- **Low-altitude cloudiness:** The clouds are at relatively low altitudes, mainly consisting of liquid water droplets. With the increase in altitude, the fraction of the ice phase increases. These low altitude clouds have relatively thicker optical depth and can reflect a large fraction of solar radiation while they do not trap terrestrial radiation on the Earth; therefore, the low altitude clouds have an overall cooling effect.
- **High-altitude cloudiness:** Clouds at high altitudes are usually composed of ice crystals. These high-altitude ice clouds are generally thin in optical depth and partially transparent to the radiation from the sun. They are known to scatter a small fraction of solar radiation, leading to a net positive RF. With the increase in altitude, the RF effects of ice clouds are known to be stronger as the ice crystal concentrations rise due to lower temperatures.

The aviation industry is known to contribute up to about 4% of total global RF from human activities. Compared to carbon dioxide (CO_2), which can accumulate in the atmosphere and exist for hundreds of years, contrails have significantly shorter lifespans, which could range from a few minutes to several hours, depending on the prevailing conditions, and in turn contribute to cloudiness [4]. Aircraft-induced cloudiness (AIC) contributes to more than half of the aviation-derived RF, exceeding the contribution from CO_2. Within the categorisation of AIC RF, the contribution from contrail cirrus is considered to be dominant. Contrail cirrus can be observed by satellites from space [2, 5, 6], further emphasising its size and consequent potential to affect the global radiation budget. RF attributed to contrail cirrus in 2006 and extrapolated predictions for 2050 are presented in Ref. [3]. The global RF induced by air traffic in the year 2006 is estimated to be $49mW/m^2$. The global flight distance in 2050 is estimated to be four times that in 2006, while the RF three times [3]. In this simulation, aircraft technology is assumed to be improved in the time period through improved propulsion efficiency and the utilisation of sustainable

https://doi.org/10.1017/aer.2024.22 Published online by Cambridge University Press

alternative fuels. Therefore, assuming a reduction of soot emission by 50% and a slight increase in the water emission index, the global RF attributed to AIC is estimated to be of 137mW/m^2 in 2050. Estimates of the different aviation-induced climate forcing terms between 2000-2018 are given in Ref. [7]. The effective radiative forcing (ERF) of contrail cirrus accounts for most of the net aviation-induced ERF, followed by aviation-emitted CO_2 accumulated from 1940 to 2018.

2.0 Literature review

2.1 Contrail formation process

Water vapour and particles in aero engine exhaust can give rise to contrails in the wake of aircrafts and are essentially formed of ice crystals. The evolution of aircraft wakes can be categorised into four regimes [8]: Jet, Vortex, Dissipation and Diffusion regimes, while the formation process of ice crystals can be divided into four stages [4].

In the jet regime, ice crystal formation is known to occur in two stages. A pair of vortices are induced by the aircraft wingtips, trapping most of the engine exhaust, referred to as the 'primary wake'. During the turbulent mixing process of engine exhaust and the ambient air, ambient aerosol particles and particulate matter are also entrained in engine plumes, along with soot particles and ultrafine aqueous particles formed in the exhaust. Due to cooling effect of the mixing process, the water vapour becomes supersaturated with respect to liquid water, forming water droplets on the particles and depending on the ambient temperature could freeze thus forming ice particles.

The ice crystals then continue to develop through two further formation stages in the vortex regime. During the vortex regime, due to the mutually induced downward velocity, the vortex pair are known to descend to a lower altitude (several hundred metres). The vortex pair then induces a secondary wake, which moves upward and carries with it a part of the exhaust and ice crystals. At the beginning of the vortex regime, ice crystals formed in the jet regime perform fast growth by absorbing more ice-supersaturated water vapour from the atmosphere, presenting a visible contrail. With the downward movement of the vortex pair, ice crystals sublimate at the lower wake due to a higher temperature. Ice crystals at the upper wake continue to grow by absorbing ice-supersaturated water vapour from the entrained ambient air.

A few minutes later, the wake does not retain its structure and enters the dissipation regime, resulting in the break-up of the vortices and mixing of the wake flow with the ambient air. Ice crystals at lower altitudes sublimate due to warmer temperatures, while those entrapped in the secondary wake region last for significantly longer periods due to lower ambient temperature at higher altitudes.

The diffusion regime normally occurs within a few hours. The contrails could spread vertically and horizontally, forming contrail cirrus, and covering large areas. These processes are known to be strongly affected by wind shear, atmospheric turbulence, particulate sedimentation, and radiative processes.

2.2 Contrail formation criteria

The formation process of contrails can be indicated on the water phase diagram. For temperatures over 273.15K, the water phase diagram is shown in Fig. 1.

The horizontal and vertical axes are the temperature and partial pressure of the water vapour, respectively. The blue curve stands for the water vapour saturation pressure over liquid water. In the region above the liquid water saturation curve, the water vapour partial pressure is higher than the corresponding water vapour saturation pressure (supersaturated), leading to water vapour condensation. Below the curve, the water vapour is considered to subsaturated, which means water remains in the gaseous phase. As can be seen in Fig. 1, at constant water vapour partial pressure condition, the water would be converted to liquid form at a certain temperature. This point of phase change for that condition is demarcated by the liquid water saturation curve. Similarly, if water were to exist in liquid form at a constant partial vapour pressure, any increase in temperature over that specified by the liquid water saturation curve would result in the water converted to vapour form.

https://doi.org/10.1017/aer.2024.22 Published online by Cambridge University Press

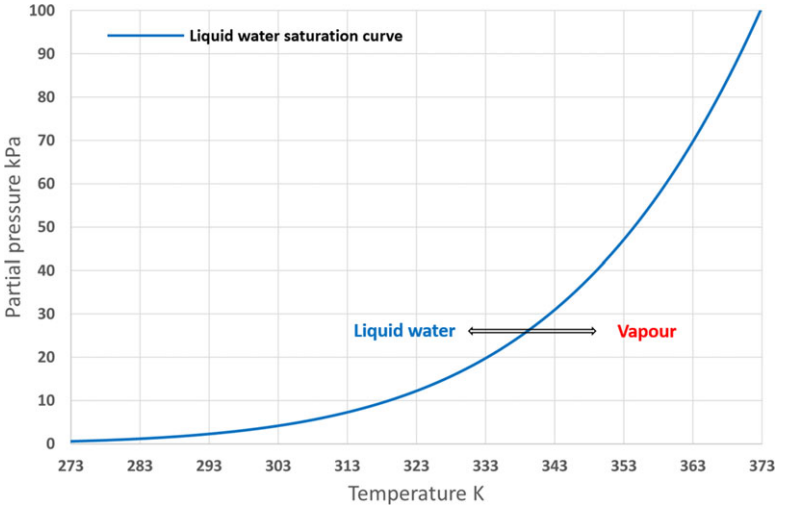

Figure 1. *Water phase diagram (above 273.15K).*

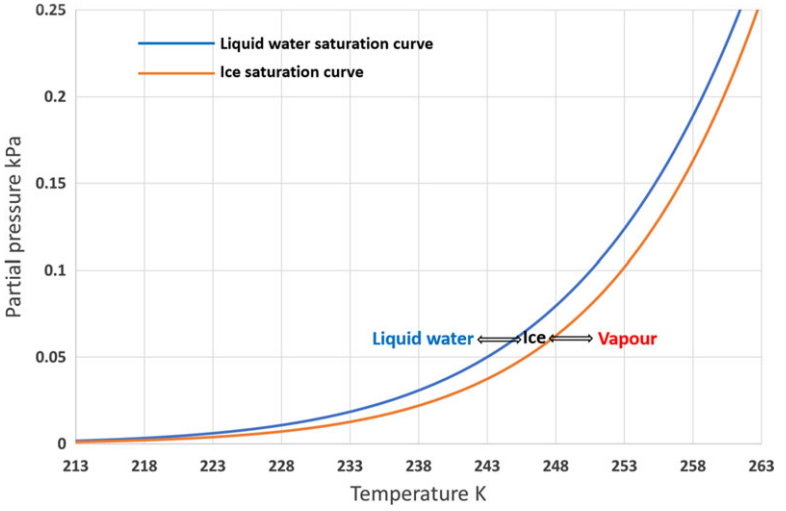

Figure 2. *Water phase diagram (below 273.15K).*

The water vapour saturation pressure is a function of static temperature. When the temperature is below 273.15K, there are three phases of water on the diagram, as shown in Fig. 2.

The blue curve stands for the water vapour saturation pressure with respect to liquid water, while the orange curve represents the water vapour saturation pressure with respect to ice. For gaseous water with constant partial pressure, with the reduction of temperature, the vapour firstly condenses into solid phase and then becomes liquid water.

For contrails, as shown in Fig. 3, point A represents the ambient water vapour condition, point B represents the water vapour condition at the engine exit. The engine exhaust is not uniform, consisting of the hot and moist core gas and relatively cold and dry bypass air; therefore, point B is the condition that the core gas and bypass air are assumed to mix homogeneously.

The line from B to A represents a hypothetical line representing the cooling and dilution process of the engine plume achieved through mixing with cooler (and drier) ambient air. This process is assumed to be adiabatic and vapour conserving; the vapour and heat are assumed to diffuse at the same rate. Therefore, the mixing line BA is represented as a straight line on the water phase diagram. From B to A,

https://doi.org/10.1017/aer.2024.22 Published online by Cambridge University Press

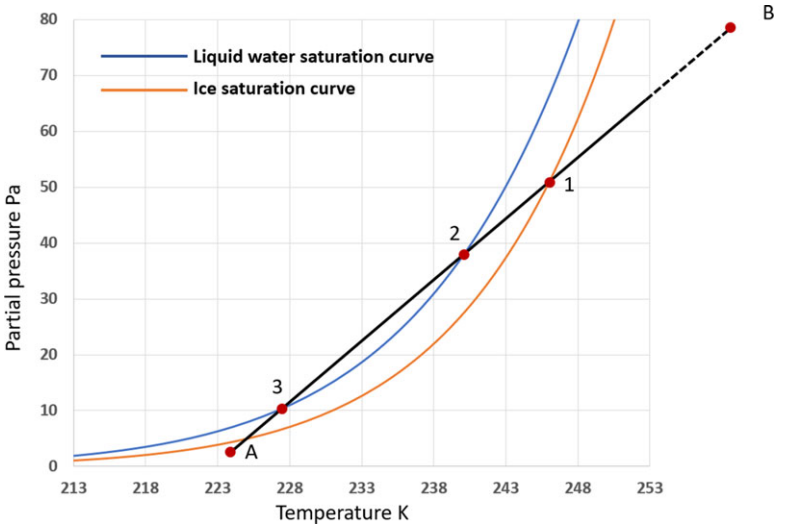

Figure 3. *Non-persistent contrail formation process.*

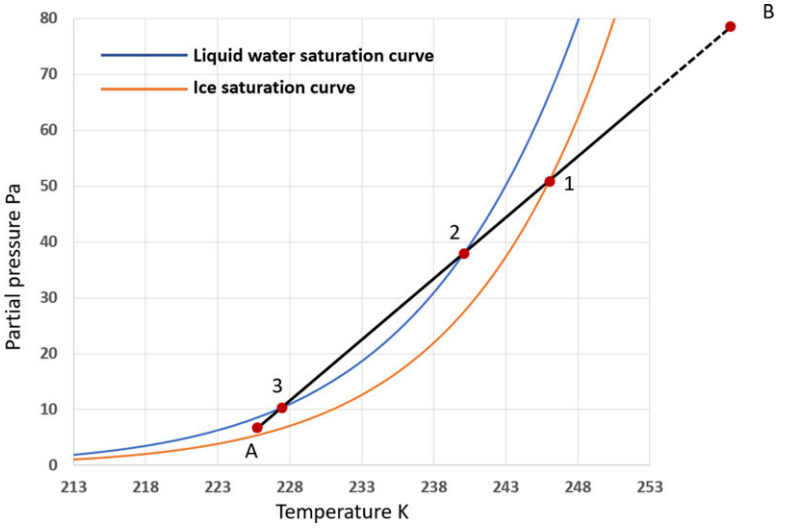

Figure 4. *Persistent contrail formation process.*

the mixing line first crosses the ice saturation curve at point 1 and then crosses the liquid water saturation curve at point 2. Before point 1, the water vapour in the plume is subsaturated. Between points 1 and 2, the water vapour becomes ice-supersaturated, but ice crystals do not form due to the lack of nucleation process. After point 2, the water vapour is liquid-water-supersaturated, condensing on the nucleation agents in the plume and forming water droplets. With the further mixing of engine plume and ambient air, the mixing line crosses the liquid water saturation curve again at point 3. After point 3, the water droplets start to freeze because of the ice-supersaturated condition; ice crystals form at this stage.

Finally, the mixing line ends at the ambient condition point. In Fig. 3, the ambient condition is subsaturated, so ice crystals sublimate soon, resulting in non-persistent contrails.

If point A is between the liquid water saturation curve and ice saturation curve, as shown in Fig. 4, the ambient condition is ice supersaturated. In an ice-supersaturated region, once contrails form, ice crystals can last for a long time, leading to persistent contrails.

https://doi.org/10.1017/aer.2024.22 Published online by Cambridge University Press

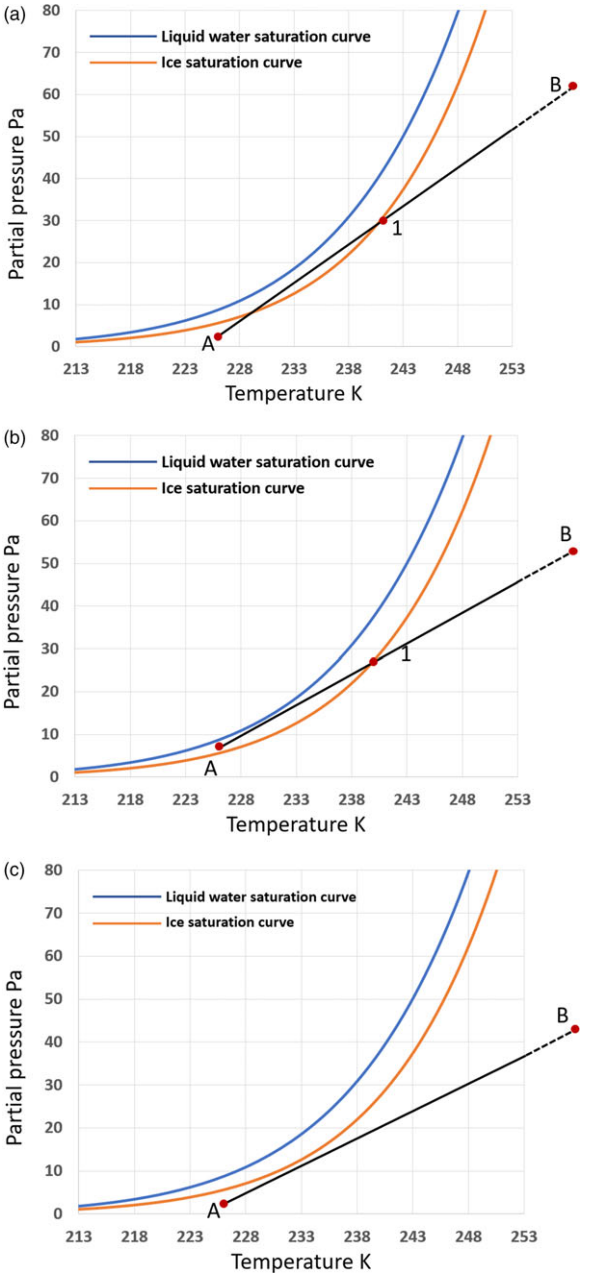

Figure 5. *No contrail formation.*

In the three cases in Fig. 5, contrails do not form. In (a) and (b), the mixing line crosses the ice saturation curve at point 1; the water vapour becomes ice supersaturated. However, without the emergence of water droplets, ice crystals cannot form; therefore, no contrail can form no matter the ambient condition is subsaturated (case (a)) or ice-supersaturated (case (b)). In case (c), the whole mixing process is subsaturated, so contrails cannot form.

In brief, on the water phase diagram, if the mixing line crosses the liquid water saturation curve, contrails form. Once contrails form, if the ambient condition is supersaturated, contrails are persistent; if the ambient condition is subsaturated, contrails are non-persistent.

https://doi.org/10.1017/aer.2024.22 Published online by Cambridge University Press

2.3 Contrail prediction model: Schmidt-Appleman criterion

Based on Section 2.2, a contrail prediction model is summarised, called the Schmidt-Appleman criterion. The slope of the mixing line can be calculated if the engine performance data and the ambient conditions are known. Once the slope of the mixing line is confirmed, a threshold temperature can be defined; if the ambient temperature is lower than the threshold temperature, contrails form; otherwise, contrails do not form.

Point B stands for the water vapour condition at the engine exhaust and point A stands for the ambient water vapour condition. The mixing line BA is straight, so its slope can be defined as [9, 10]:

$$G = \frac{c_P \cdot EI_{H_2O} \cdot p}{\varepsilon(1-\eta)Q} \tag{1}$$

Where:

- p is the air pressure
- ε is the ratio of molar masses of water and air
- Q is the lower heat value (LHV) of the fuel (amount of heat produced by burning a kg of fuel)
- η is the engine overall efficiency
- c_P is the specific heat capacity of air
- $\mathrm{EI_{H_2O}}$ is the water emission index of the fuel (for kerosene, the $\mathrm{EI_{H_2O}}$ is 1.26, which means the combustion of 1kg of kerosene produces 1.26kg of water)

Therefore, once the engine performance data (η, EI_{H_2O}, Q) and ambient conditions (p, c_P) are obtained, with the known constants (ε), the slope of the mixing line can be calculated. The ambient condition and the mixing line slope can confirm the position of the mixing line on the water phase diagram. Equation (1) shows the parameters that affect the mixing line slope. For a specific engine at a specific cruise altitude, the ambient pressure p, the specific heat capacity of air c_P and molar masses of water and air ε cannot be changed. For current engines using kerosene as the fuel, the fuel heat value Q cannot be changed. Therefore, only a reduction in $\mathrm{EI_{H_2O}}$ or η can lower the G, while reducing η will lead to a significant increase in specific fuel consumption (SFC), reducing $\mathrm{EI_{H_2O}}$ is the emphasis in the following study.

$\mathrm{EI_{H_2O}}$ is the water emission index of the fuel; from a contrail mitigation perspective, the $\mathrm{EI_{H_2O}}$ can represent the water content in the exhaust gas at the exhaust nozzle exit plane. Therefore, by removing water content from the exhaust gas before discharging, $\mathrm{EI_{H_2O}}$ can be reduced. By applying the Schmidt-Appleman criterion, required water removal for contrail mitigation at different ambient relative humidity (RH) can be calculated for a specific engine. A threshold condition can be defined when the mixing line touches the liquid water saturation curve at the tangential point, which is named the liquid maximum (LM) point (Fig. 6). The LM point can be confirmed by the following equations [9]:

$$\frac{de_{sat,l}(T_{LM})}{dT_{LM}} = G \tag{2}$$

$$e_{LM} = e_{sat,l}(T_{LM}) \tag{3}$$

For a specific G, the corresponding threshold mixing line can be confirmed on the water phase diagram if LM is obtained. As indicated in Fig. 7, If the actual mixing line (the solid line) is at the left side of the threshold mixing line (the dotted line), the actual mixing line must cross the liquid water saturation curve, which means contrails form; if the actual mixing line (the dashed line) is at the right side, contrails do not form.

The threshold ambient condition point liquid critical (LC) is defined on the threshold mixing line, between the LM point and the horizontal axis; its position is determined by the ambient RH [9]:

https://doi.org/10.1017/aer.2024.22 Published online by Cambridge University Press

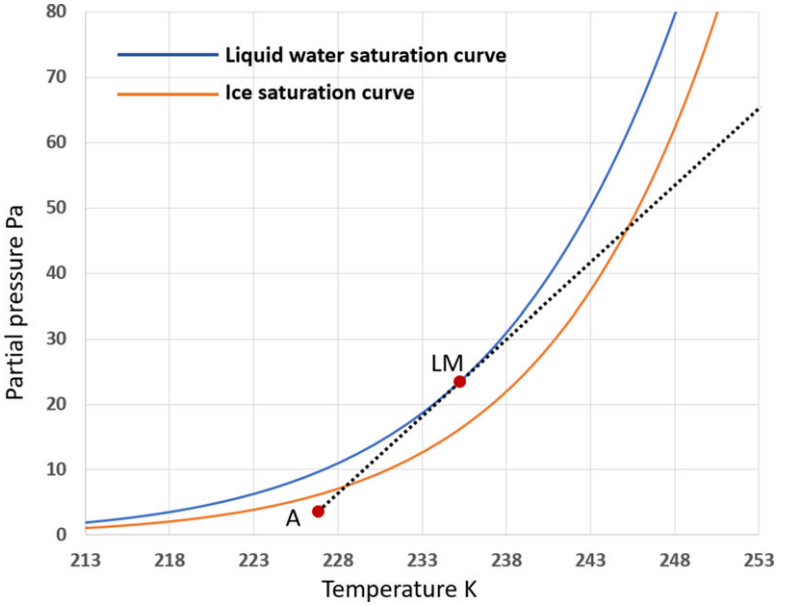

Figure 6. *The threshold condition.*

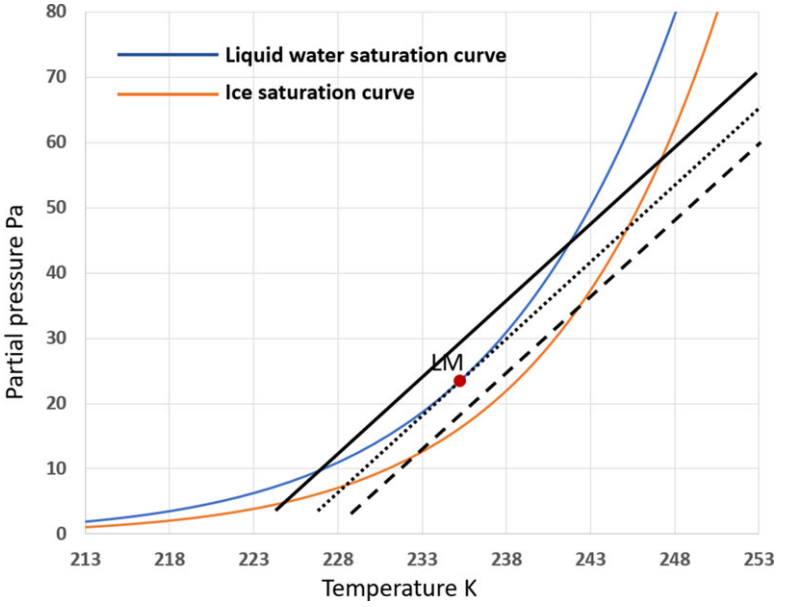

Figure 7. *Using threshold condition to predict contrail formation.*

$$T_{LC} = T_{LM} - \frac{e_{sat,l}\,(T_{LM}) - RH \cdot e_{sat,l}\,(T_{LC})}{G} \tag{4}$$

$$e_{LC} = RH \cdot e_{sat,l}\,(T_{LC}) \tag{5}$$

As shown in Fig. 8, for example, when the ambient RH is 50%, the LC point is the crossing point of the threshold mixing line and the 50% RH curve (the grey curve, $e = 50\% \cdot e_{sat,l}\,(T)$). The liquid

https://doi.org/10.1017/aer.2024.22 Published online by Cambridge University Press

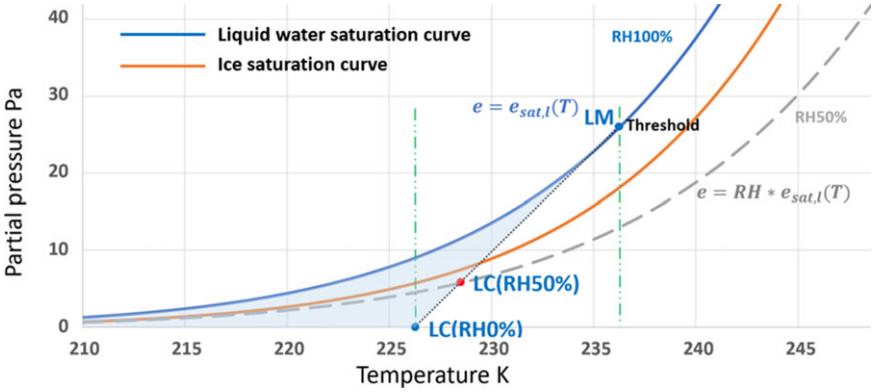

Figure 8. *The threshold ambient condition.*

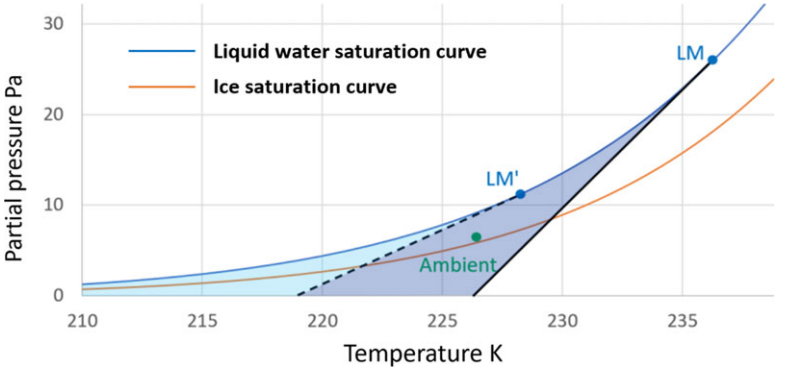

Figure 9. *Mixing line slope's impact on contrail formation.*

water saturation curve is the 100% RH curve; thus, the LM point is the LC point when the ambient RH is 100%. The threshold mixing line, the liquid water saturation curve and the horizontal axis form a contrail zone, shown in Fig. 8 as a light blue zone. If the ambient condition point falls in the contrail zone, the actual mixing line must be at the left side of the threshold mixing line, crossing the liquid water saturation curve, which means contrail formation. If the ambient temperature is lower than the T_{LC}, the ambient point is in the contrail zone; otherwise, it is out of the contrail zone, which means no contrail formation.

In brief, the contrail prediction model is simplified as a comparison between the ambient temperature and corresponding RH-based threshold temperatures. If $T_a > T_{LC}$, contrails do not form; if $T_a < T_{LC}$, contrails form.

Figure 9 shows two different mixing lines. The solid line has a higher slope, forming a larger contrail area (dark blue area + light blue area), covering the ambient condition point, so contrails form. The dashed line has a lower slope and a smaller contrail area (light blue area), which cannot cover the ambient condition point, and contrails will not form. Therefore, a lower mixing line slope tends to reduce the possibility of contrail formation.

3.0 Methodology

According to the discussion above, a reduction in EI_{H_2O} to mitigate contrail formation is reflected by the reduction of the slope of the mixing line. Therefore, for an aircraft flying at a specific altitude, only

https://doi.org/10.1017/aer.2024.22 Published online by Cambridge University Press

Table 1. *Simulation cases*

	Ambient RH = 0	Ambient RH = 50%	Ambient RH = 75%
Water removal = 0	Case 1	Case 2	Case 3
Water removal = 40%	Case 4	Case 5	Case 6
Water removal = 70%	Case 7	Case 8	Case 9

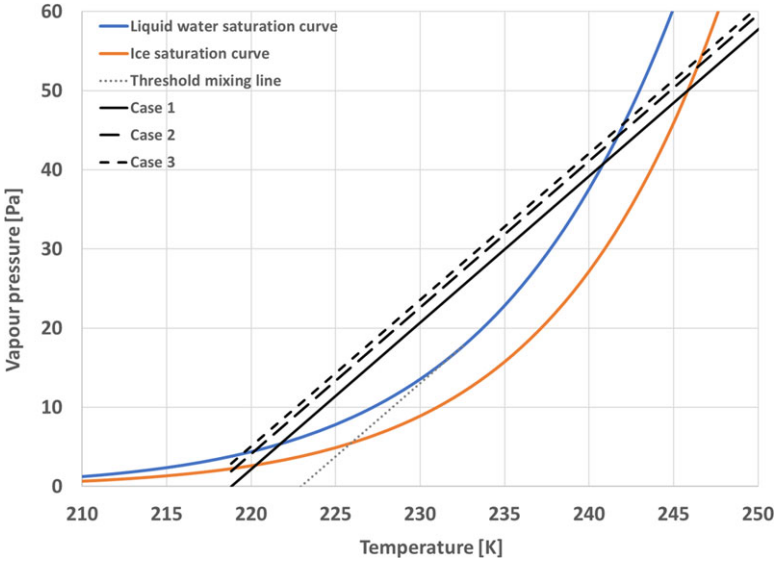

Figure 10. *Cases 1, 2, and 3.*

EI_{H_2O} and ambient RH can affect the formation of contrails. EI_{H_2O} determines the slope of the mixing line, while the ambient RH defines the position of the ambient condition point on the water phase diagram. To explore the percentage of water extraction's impact on contrail mitigation, nine different cases have been considered, depending on combinations of the water removal percentage and ambient RH (Table 1). The baseline engine is inspired by the architecture and performance characteristics of the leading edge aviation propulsion (LEAP) 1-A, as shown in the Appendix A.

For these conditions the Schmidt-Appleman criterion is applied, and the simulation results are plotted on the water phase diagram.

Examining the cases which no water is extracted (cases 1, 2 and 3), it is found that contrails are formed irrespective of the ambient RH condition as their mixing lines have the same slope (which is 1.85), and they all cross the water saturation curve (Fig. 10). However, ambient conditions in cases 1 and 2 are ice-subsaturated, which means contrails are non-persistent; while the ambient condition in case 3 is ice-supersaturated, so contrails are persistent.

When 40% water vapour is removed from the exhaust gas (cases 4, 5 and 6), the mixing lines slope is reduced from 1.85 to 1.11. As a result, when the RH is 0% (dry air – case 4) contrails do not form as the mixing line no longer crosses the water saturation curve (Fig. 11). When RH increases to 50% (case 5) and 75% (case 6) contrails will form. However, due to the different ambient RHs, contrails are non-persistent in case 5 but persistent in case 6. This is evident in Fig. 11 as the end of case 5 mixing line falls below the orange curve (which is the ice saturation curve) while the end of case 6 mixing line is above the orange curve.

When ever greater water content is extracted from the exhaust gas (70% – case 7, 8 and 9), it is found that contrails will not form irrespectively of the ambient air RH. The mixing lines slope for these cases

https://doi.org/10.1017/aer.2024.22 Published online by Cambridge University Press

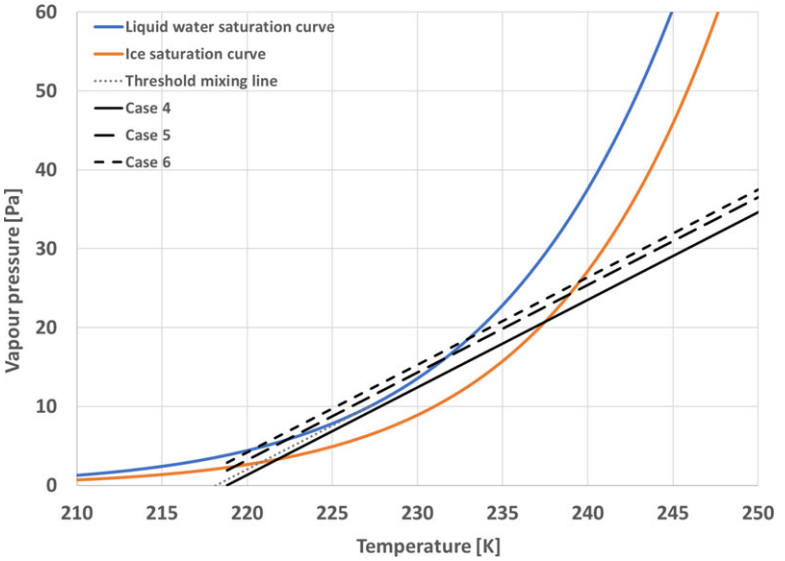

Figure 11. *Case 4, 5, and 6.*

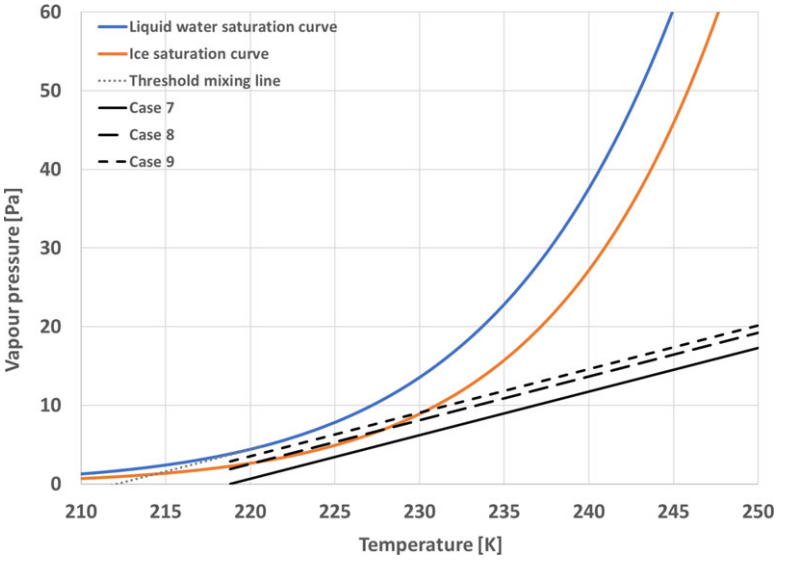

Figure 12. *Case 7, 8, and 9.*

become even lower (0.55). Therefore, they do not cross the water saturation curve making the contrail formation impossible (Fig. 12).

Comparing the results on the same ambient RH basis, it was found that at higher ambient RH, a larger amount of water should be removed from the exhaust gas for contrail mitigation. In cases 1, 4 and 7, where the ambient RH is 0 for all the cases, contrails only form when no water is extracted (case 1, Fig. 13). For 50% ambient RH (cases 2, 5 and 8), contrail formation can only be avoided when 70% water is extracted (case 8, Fig. 14) but contrails form in case 2 and case 5 are non-persistent (which is determined by the RH). When the ambient RH is high at 75%, contrail formation can also only be

https://doi.org/10.1017/aer.2024.22 Published online by Cambridge University Press

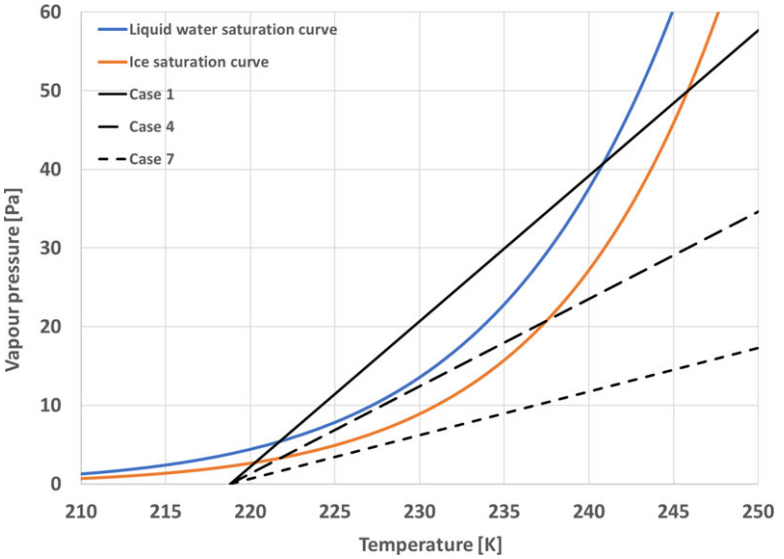

Figure 13. *Case 1, 4, and 7.*

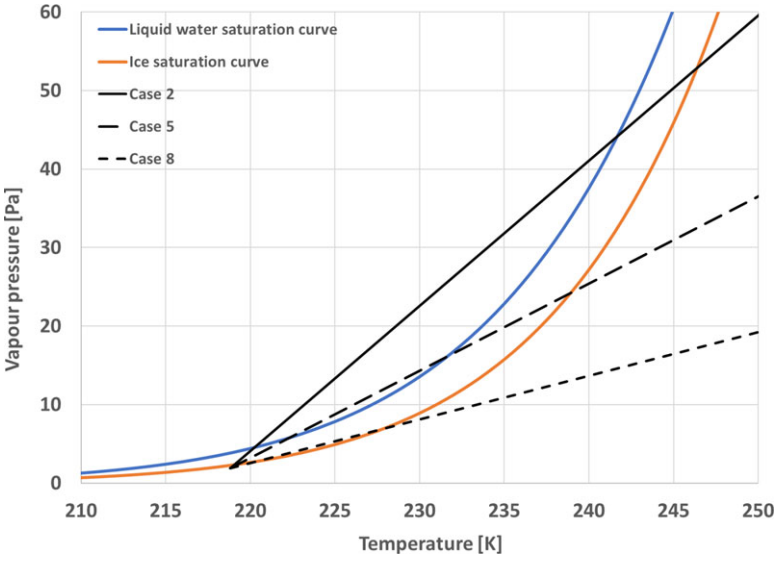

Figure 14. *Case 2, 5, and 8.*

avoided when 70% water is extracted (Fig. 15), while the contrails that form in case 3 and case 6 are persistent.

To obtain the water removal requirements for every possible ambient RH, the simulation can be applied to combinations of every percentage of water removal and ambient RH, as shown in Table 2 (totally $101 \times 101 = 10{,}201$ cases).

The simulation results can be summarised in a plot, which can give an overview of the water removal percentage for contrail mitigation for a specific engine at a specific operating condition. The following section discusses how the plot can be used for the purpose of contrail mitigation through water removal.

https://doi.org/10.1017/aer.2024.22 Published online by Cambridge University Press

Table 2. *Water removal simulation cases*

Water removal \ Ambient RH	0	1%	. . .	99%	100%
0	Case 0–0	Case 0–1	. . .	Case 0–99	Case 0–100
1%	Case 1–0	Case 1–1	. . .	Case 1–99	Case 1–100
. . .	. . .	. . .	. . .	. . .	. . .
99%	Case 99–0	Case 99–1	. . .	Case 99–99	Case 99–100
100%	Case 100–0	Case 100– 1	. . .	Case 100–99	Case 100–100

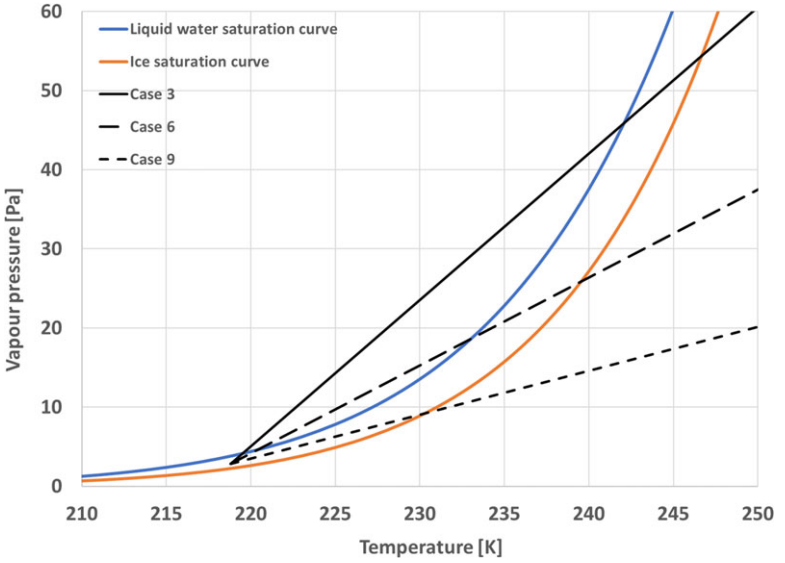

Figure 15. *Case 3, 6, and 9.*

4.0 Results

4.1 The water removal characteristic plot

The water removal characteristic plot for the baseline kerosene fuelled LEAP 1-A engine is shown in Fig. 16. Every point on the plot refers to a combination of water removal percentage and the local ambient RH. If the point falls in the dark blue area, which represents higher levels of water removal percentage, contrail will not form. If the point falls in the contrail area, which refers to the light blue area and yellow area, contrail will form. The plot can indicate the lowest water removal percentage required for the purpose of contrail mitigation.

The nine cases of Table 1 can be located on the plot. On the plot, it can be easily observed that with the increase of ambient RH, the lowest water removal percentage for contrail avoidance also increases. When the ambient RH is 0, the minimum water removal for contrail avoidance is 36%; for ambient RH = 100%, the requirement is at least 76%. However, as discussed in Section 1, only persistent contrails and cirrus contribute to the RF, so the water removal strategies only apply to conditions that enable the formation of persistent contrails, which have ambient RHs over 60%. Therefore, according to the plot, around 52–76% of water removal is required for contrail mitigation for the baseline LEAP engine depending on the ambient RH.

https://doi.org/10.1017/aer.2024.22 Published online by Cambridge University Press

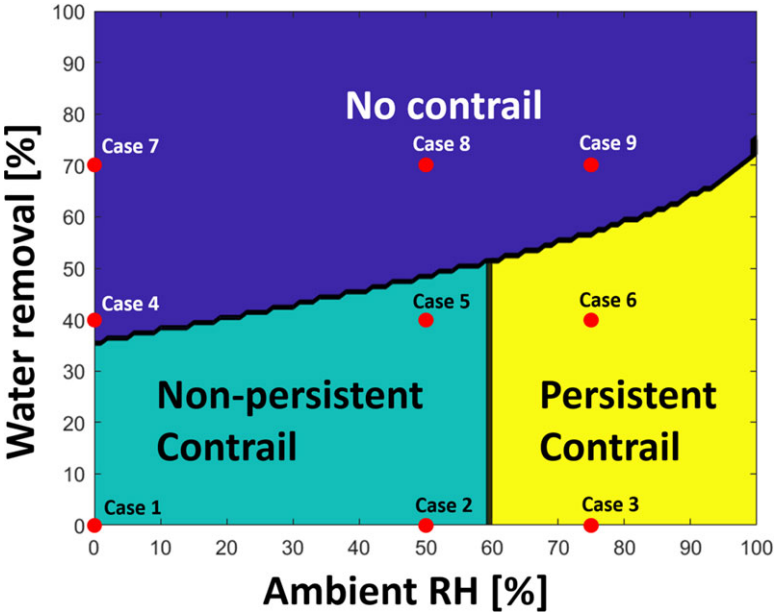

Figure 16. *Water removal characteristic plot for kerosene fuelled LEAP engine.*

4.2 The water removal characteristic plot for hydrogen fuelled engine

The utilisation of hydrogen as an aviation fuel has gained much attention in recent years. As a sustainable fuel, hydrogen has considerable potential to reduce the aviation environmental footprint. By using hydrogen as the fuel, aircraft can achieve zero-carbon and low NO_x emissions.

The water emission index of hydrogen is 9, which means the combustion of 1kg of hydrogen produces 9kg of water, while it is 1.26 for kerosene. Assuming the same combustion heat release, the water produced by the combustion of hydrogen is about 2.6 times the water produced by burning kerosene. The significant increase in water vapour emission increases the possibility of contrail formation as the mixing line slope on the water phase diagram is higher. The water removal characteristic plots of kerosene and hydrogen fuelled aircraft show significant differences. The water removal characteristic plot for hydrogen fuelled LEAP engine is shown in Fig. 17. The hydrogen fuelled engine model is designed to produce the same net thrust as the kerosene fuelled engine model.

Compared to the kerosene fuelled engine, the hydrogen fuelled engine presents a higher water removal requirement for contrail mitigation. Depending on the ambient RH, 82–91% water removal is required.

4.3 Water removal through vapour condensation

In previous sections, the fuel heat value used in the Schmidt-Appleman criterion is the LHV of the fuel, which means the heat released by burning per kg of the fuel if the water produced by the combustion process is finally in gaseous state. To extract water vapour from the engine exhaust, the most widely considered approach is to let the vapour condense, so the liquid water can be separated from the gaseous flow. The condensation process of water vapour releases latent heat, and this amount of heat is added to the aircraft plume so the utilisation of LHV in the Schmidt-Appleman criterion is no longer accurate as not all water is discharged in gaseous state. When the water product is finally in the liquid state, the heat released by burning per kg of the fuel is the higher heat value (HHV). If the percentage of water extraction is λ, finally λ of the water will be in liquid state while $(1-\lambda)$ of water will be in gaseous state;

https://doi.org/10.1017/aer.2024.22 Published online by Cambridge University Press

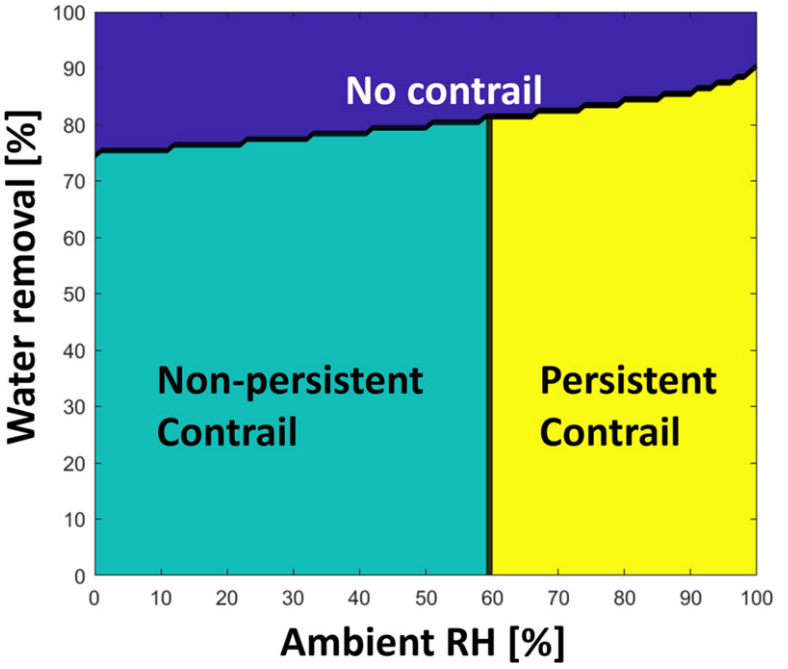

Figure 17. *Water removal characteristic plot for hydrogen fuelled LEAP engine.*

therefore, λ of the fuel burned releases the HHV and (1-λ) of the fuel burned releases the LHV. Then the fuel equivalent heat value (EHV) can be defined based on the percentage of water extraction to include the latent heat released by water condensation into consideration:

$$EHV = \lambda HHV + (1 - \lambda)\, LHV \tag{6}$$

The slope of the mixing line then becomes:

$$G = \frac{c_P \cdot EI_{H_2O} \cdot p}{\varepsilon(1 - \eta)EHV} \tag{7}$$

By using the EHV, the water removal characteristic plot for the kerosene fuelled LEAP engine is shown in Fig. 18.

The minimum required water removal percentage considering the latent heat is 51–75% depending on the ambient RH, slightly lower than the requirement in Section 4.1, which is 52–76%. The latent heat makes the EHV higher than the LHV, so the mixing line slope can be lower, which reduces the possibility of contrail formation, and hence a lower water removal requirement. Using the EHV instead of LHV, the calculation results are more accurate as the latent heat released by water vapour condensation is also considered.

4.4 Water discharging system

The design point fuel mass flow rate of the kerosene fuelled engine model is 1.074kg/s and the water emission index of kerosene is 1.26; therefore, at design point, the water mass flow rate in the exhaust flow is 1.353kg/s. According to the discussion in Section 4.1, around 52–76% of water removal is required for contrail mitigation; therefore, around 0.704–1.028kg/s of water is expected to be extracted. Similarly, for the hydrogen fuelled engine model, 3.014–3.345kg/s of water is expected to be extracted.

The water extracted from the exhaust flow is expected to be discharged immediately to the environment, because the extra weight due to water storage onboard leads to fuel burn penalty. However,

https://doi.org/10.1017/aer.2024.22 Published online by Cambridge University Press

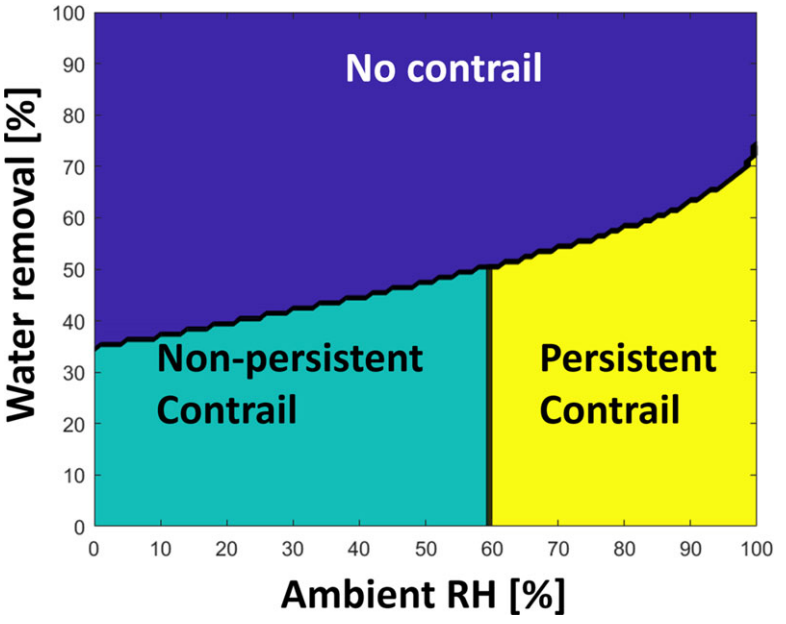

Figure 18. *Water removal characteristic plot considering the latent heat.*

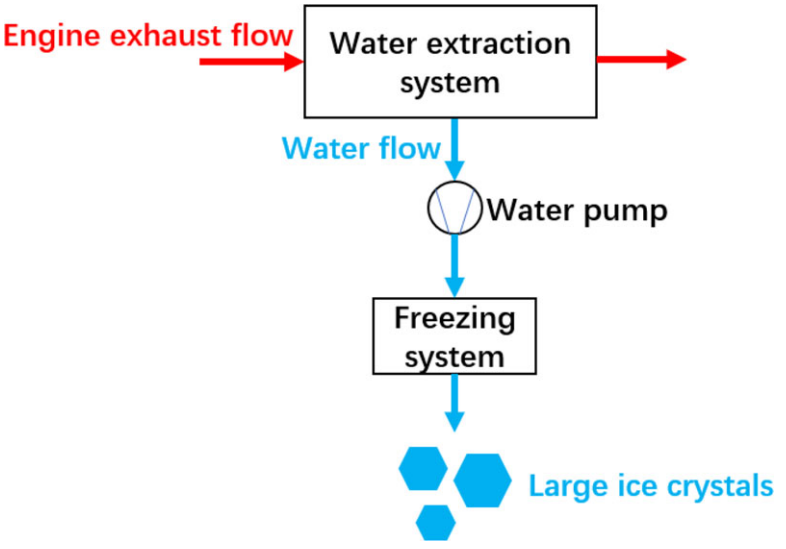

Figure 19. *Water discharging system.*

emitting liquid water may not be a good choice as the turbulence may break large water droplets into small water droplets, and the small water droplets will freeze and form contrails.

A possible choice of the water discharging system is to emit the water in the form of large ice crystals, as shown in Fig. 19. The extracted water is transferred to a freezing system by a pump. In the freezing system, the water freezes and forms large ice crystals. Once the large ice crystals are emitted, they will not stay at high altitude but sediment soon, so contrail formation can be prevented.

https://doi.org/10.1017/aer.2024.22 Published online by Cambridge University Press

5.0 Conclusions

According to the Schmidt-Appleman criterion, the slope of the mixing line is highly related to the possibility of contrail formation. Higher mixing line slopes correspond to higher contrail formation threshold temperatures, hence higher possibilities of contrail formation. To reduce the mixing line slope for contrail mitigation at a given cruise altitude, either a reduction in the engine efficiency or the water emission index should be achieved; however, reducing the engine efficiency is not acceptable as it will drastically increase SFC, so extracting water from the engine exhaust to reduce the water emission index becomes a promising choice.

The minimum required water removal from the engine exhaust for contrail mitigation is simulated and discussed in this paper. For the baseline LEAP 1-A model burning kerosene as the fuel, to prevent contrail formation, at least 36% of water in the exhaust should be removed when the ambient RH is 0 while 76% of water should be removed when the ambient RH is 100%. The water removal requirement increases with the increase of ambient RH. At 35,000ft, which is the cruise altitude of the engine model, persistent contrails only form when the ambient RH is higher than 60% while non-persistent contrails almost have no contribution to the global RF, so water removal is only applied to RH from 60 to 100% and the corresponding water removal percentage is 52–76%.

For the LEAP 1-A engine model using hydrogen as the fuel and producing the same net thrust as the kerosene fuelled model, much more water should be removed for contrail mitigation. When the ambient RH varies from 60 to 100%, the minimum water removal percentage requirements increase from 82 to 91%, much higher than that of the kerosene fuelled model.

If the water in the exhaust flow is extracted in liquid state, the latent heat released by water vapour condensation could not be ignored as it adds additional heat to the engine exhaust and affects the slope of the mixing line. Considering the latent heat release, the water removal requirement is 51–75% for kerosene fuelled engine model when the ambient RH is 60–100%, slightly lower than the simulation without considering the latent heat, which is 52–76%. The latent heat release lowers the mixing line slope and reduces the possibility of contrail formation.

Competing interests. The authors declare none.

References

[1] World Meteorological Organization (WMO). Aircraft condensation trails | International Cloud Atlas, Available at: https://cloudatlas.wmo.int/en/aircraft-condensation-trails.html (Accessed: 1 January 2022), 2017.
[2] NASA. The Evolution of a Contrail, Available at: https://earthobservatory.nasa.gov/images/78154/the-evolution-of-a-contrail (Accessed: 1 January 2022), 2012.
[3] Bock, L. and Burkhardt, U. Contrail cirrus radiative forcing for future air traffic, *Atmos. Chem. Phys.*, 27 June 2019, doi: 10.5194/acp-19-8163-2019
[4] Kärcher, B. Formation and radiative forcing of contrail cirrus, Nature Communications. Nature Publishing Group, 2018, doi: 10.1038/s41467-018-04068-0
[5] Iwabuchi, H., Yang, P., Liou, K.N. and Minnis P. Physical and optical properties of persistent contrails: Climatology and interpretation, *J. Geophys. Res. Atmos.*, 2012, doi: 10.1029/2011JD017020
[6] Tesche, M., Achtert, P., Glantz, P. and Noone, K.J. Aviation effects on already-existing cirrus clouds, Nature Communications. Nature Publishing Group, 2016, doi: 10.1038/ncomms12016
[7] Lee, D.S., Fahey, D.W., Skowron, A., Allen, M.R., Burkhardt, U., Chen, Q., et al. The contribution of global aviation to anthropogenic climate forcing for 2000 to 2018, *Atmos. Environ.*, doi: 10.1016/j.atmosenv
[8] Paoli, R. and Shariff, K. Contrail modeling and simulation, Annual Review of Fluid Mechanics. Annual Reviews Inc., 3 January 2016, doi: 10.1146/annurev-fluid-010814-013619.
[9] Schumann, U. On conditions for contrail formation from aircraft exhausts, Meteorologische Zeitschrift, 1996, doi: 10.1127/metz/5/1996/4
[10] Gierens, K. Physical fundamentals of contrail formation, the Schmidt-Appleman criterion, and the role of particles, FORUM-AE Second Workshop, 2014.

https://doi.org/10.1017/aer.2024.22 Published online by Cambridge University Press

Appendix

Table A.1 *Cranfield University (CU) LEAP 1-A engine model design point performance data*

Altitude	0ft
Mach number	0
Bypass ratio	10.5
Fan PR	1.56
Fan efficiency	89.5%
Booster compressor PR	1.24
Booster compressor efficiency	90.4%
HPC PR	20
HPC efficiency	90.8%
HPT efficiency	91.5%
LPT efficiency	92.6%
TET	1,850K
Intake mass flow rate	505.2kg/s
Combustor cooling bleed	0.08

Table A.2 *Kerosene-fuelled engine model simulation results*

Cruise altitude	35,000ft
Mach number	0.8
Ambient pressure	23.8kPa
Ambient temperature	218.81K
Fuel mass flow rate	0.333kg/s
Engine net thrust	23.7kN
True air speed (TAS)	237.3m/s

Table A.3 *Hydrogen-fuelled engine model simulation results*

Cruise altitude	35,000ft
Mach number	0.8
Ambient pressure	23.8kPa
Ambient temperature	218.81K
Fuel mass flow rate	0.112kg/s
Engine net thrust	23.7kN
TAS	237.3m/s

Cite this article: Gao X., Isoldi A., Nalianda D. and Nikolaidis T. (2024). Water extraction in aero gas turbines for contrail mitigation. *The Aeronautical Journal*, **128**, 1344–1361. https://doi.org/10.1017/aer.2024.22